Hindawi
International Journal of Photoenergy
Volume 2021, Article ID 4343203, 20 pages
https://doi.org/10.1155/2021/4343203

Review Article

Parameter Estimation of the Photovoltaic System Using Bald Eagle Search (BES) Algorithm

Ndongmo Fotsa Nicaire,[1] **Perabi Ngoffe Steve**,[1] **Ndjakomo Essiane Salome**,[1,2] **and Abessolo Ondoua Grégroire**[3]

[1]*Laboratory of Applied Science Technology (LTSA), University of Douala, Cameroon*
[2]*Higher Technical Teacher Training College of Ebolowa, University of Yaounde 1, Cameroon*
[3]*Ecosystems and Fisheries Resources Laboratory, University of Douala, Cameroon*

Correspondence should be addressed to Ndongmo Fotsa Nicaire; dfnicaire@yahoo.fr

Received 28 June 2021; Revised 23 September 2021; Accepted 18 October 2021; Published 31 October 2021

Academic Editor: Francesco Riganti-Fulginei

The global demand for renewable energy is growing, and one of the proposed solutions to this energy crisis is the use of photovoltaic systems. So far, they are a reliable solution, as they are nonpolluting and can be used almost anywhere on the planet. However, the design and development of more efficient photovoltaic cells and modules require an accurate extraction of their intrinsic parameters. Up to date, metaheuristic algorithms have proven to be the best methods to obtain accurate values of these intrinsic parameters. Hence, to extract these parameters reliably and accurately, this paper presents an optimization method based on the principle of bald eagle search (BES) during fish hunting. This search is divided into three steps: in the first stage (space selection), the eagle selects the space with the largest number of prey; in the second stage (space search), the eagle moves into the selected space to search for prey; in the third stage (dive), the eagle swings from the best position identified in the second stage and determines the best point to hunt. Thus, we used the proposed BES algorithm to determine the parameters of the single-diode model (SDM), the double-diode model (DDM), and the PV modules. This algorithm converges very quickly and gives a root mean square error (RMSE) of $9.8602e-04$ for the single-diode model and $9.8248e-4$ for the dual-diode model. The results obtained show that the proposed algorithm is more efficient than the other methods available in the literature, in terms of the better accuracy of the results obtained. The good harmony of the I-V and P-V characteristic curve of the calculated parameters with that of the measured data from a PV module/cell data sheet proves that the proposed BES should be used among the methods provided in the literature for the identification of PV solar cell parameters.

1. Introduction

The energy demand of almost every country in the world is increasing due to its large-scale industrial expansion, population growth, and the continuous growth of per capita energy consumption. It is worth noting that most of the energy needs are in the form of electricity. In contrast, the use of fossil fuel-based electricity generation has reached saturation levels due to increased environmental concerns and limited resources. Thus, the gaps between demand and production in the future must be filled by renewable energy sources [1]. However, as the solar energy obtained from a solar PV module is not constant, a major challenge is therefore to maximise the use of solar energy due to the unpredictability of the power output of PV modules caused by the resulting variations in irradiance levels and cell temperature [2]. Thus, the competition to optimize and increase the efficiency of photovoltaic cells has led researchers to find

methods to determine the intrinsic parameters of these cells. In the literature review, several methods have been proposed for the extraction of the parameters; each of these methods has drawbacks, either in terms of complexity of use and accuracy or in terms of convergence and speed. These methods are classified into three categories: analytical, numerical, and metaheuristic methods [3].

In the analytical method, a set of transcendental equations is solved to estimate the parameters of the solar cell. The main advantage of the analytical method is the speed of calculation and relatively accurate results. Analytical methods are simple, with a short computation time. Sometimes, a single iteration is sufficient to obtain the result [4]. Although this approach is very popular, it is not always easy to apply. In addition, they need many data points of the I-V curve, which in turn complicates the computation [5]. Analytical methods include Lambert's W function [6], Taylor series expansion [7], and Chebyshev polynomials [8, 9]. Some of these methods estimate 5 parameters, and others extract only the series and shunt resistance. The main weakness of analytical methods is that they are only suitable for standard conditions; consequently, they have poor results with variable ambient conditions [10]. Numerical methods with curve-fitting techniques are better than analytical methods. The algorithms of these methods provide accurate results by evaluating all points of the PV-IV curves using the algorithm [10].

Metaheuristic algorithms are global optimization techniques which do not impose any restrictions on the problem formulation and have the ability to solve various complex problems [11]. In the literature, many metaheuristic algorithms have been suggested for extracting the parameters of PV solar cell models, such as the Genetic Algorithm (GA) [12, 13], the Cuckoo Search (CS) Algorithm [11, 14], Particle Swarm Optimization (PSO) [15–17], Differential Evolution (DE) algorithm [18], Artificial Bee Colony (ABC) algorithm [19–21], Artificial Algorithm of Bee Swarm Optimization (ABSO) [22], Bacterial Foraging Optimization (BFO) algorithm [23, 24], Biogeography-Based Optimization (BBO) algorithm [25], Floral Pollination Algorithm (FPA) [26, 27], Jaya Optimization Algorithm (JAYA) [28, 29], Salp Swarm Algorithm (SSA) [30], Bird Mating Optimization (BMO) algorithm [31], Teaching-Learning-Based Algorithm (TLBO) [20, 32–34], Whale Optimization Algorithm (WOA) [35–37], Backtracking Search Algorithm (BSA) [38], Sine-Cosine Algorithm (SCA) [39], Imperialist Competitive Algorithm (ICA) [40, 41], Multiverse Optimizer (MVO) algorithm [42], Ant-Lion Optimizer (ALO) algorithm [43, 44], Eagle Strategy (ES) [45], Cat Swarm Optimization (CSO) [46], Harmony Search (HS) [47], Firefly Algorithm (FA) [48], Simplified Swarm Optimization (SSO) [49], Moth-Flame Optimization (MFO) algorithm [50], Water Cycle Algorithm (WCA) [51], Enhanced Vibration of Particles System (EVPS) [52], Harris Hawks Optimization (HHO) [53], Shuffled Frog Leaping (SFL) algorithm [54], Metaphor-Free Dynamic Spherical Evolution (DSCE) [55], enhanced metaphor-free gradient-based optimizer (EGBO) [56], delayed dynamic step shuffling frog-leaping algorithm (DDSFLA) [57], evolutionary shuffled frog leaping with memory pool (SFLBS) [58], enhanced spherical evolution (LCNMSE) [59], random reselection particle swarm optimization (PSOCS) [60], boosting slime mould algorithm (CNMSMA) [61], and Teaching-Learning Artificial-Based Bee Colony (TLABC) [20]. Comparative with analytical and numerical approaches, these metaheuristic algorithms were able to provide satisfactory results for the extraction of PV model parameters. However, these metaheuristic algorithms still have inherent drawbacks. For example, HS is very sensitive to the initial population, PSO is easily subjected to premature convergence, ABC is poor when the system is in operation, and CS suffers from slow convergence [11].

This paper presents a comprehensive study on the estimation of design parameters for SDM, DDM, and PV modules using the bald eagle search (BES) algorithm [62]. The paper is organised as follows: Section 1, introduction; Section 2, mathematical models and analysis of different models for cells, modules, and PV; Section 3, illustration of the formulation and optimization problem of models; in Section 4, we present the methodology for applying the optimization algorithm to estimate the model parameters; Section 4 presents the results and discussions and finally we conclude the paper.

The main contribution of our work is that we are proposing a new algorithm (BES) to extract the parameters of different cell models (single diode, double diode) and photovoltaic panels. Comparisons were made between the BES and the different algorithms on the extraction of the parameters of the three models. Comparing the results obtained using BES with those obtained through other methods, the accuracy and the reliability of the results can be clearly observed. Thus, BES can be an effective alternative for the parameter extraction from PV models.

2. Photovoltaic Model Description

In practical applications, a single-diode model (SDM) and double-diode model (DDM) are commonly used to describe the nonlinear voltage–current characteristics of photovoltaic systems. This section describes the properties of each of these two models [3, 52, 57].

2.1. Single-Diode Model. The single-diode model is shown in Figure 1. This model is the most used in many researches and better than the two-diode models (described after) due to its behaviour which is closer to a PV cell than the series resistance model (simplified) and its simplicity for the mathematical calculation [29].

$$I = I_{\mathrm{ph}} - I_{\mathrm{d}} - I_{\mathrm{sh}}, \tag{1}$$

$$I_{\mathrm{sh}} = \frac{V + R_{\mathrm{s}} \times I}{R_{\mathrm{sh}}}, \tag{2}$$

$$I = I_{\mathrm{ph}} - I_{\mathrm{sd}}\left(\exp\left(\frac{q(V + R_{\mathrm{s}} \times I)}{n \times K \times T}\right) - 1\right) - \frac{V + R_{\mathrm{s}} \times I}{R_{\mathrm{sh}}}, \tag{3}$$

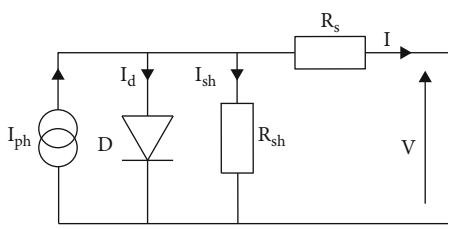

Figure 1: Single-diode equivalent model.

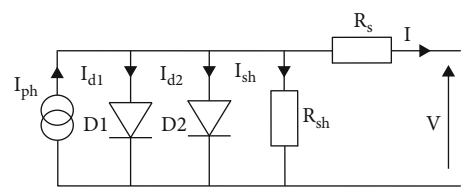

Figure 2: Equivalent model with two diodes.

with I_d as the saturation current of the diode, q the charge of one electron ($q = 1.60217646 \times 10^{-19}$C), n the ideality factor of the diode, K Boltzmann's constant ($K = 1.3806503 \times 10^{-23}$J/K), and T the temperature in Kelvin.

The equation model (3) is also called the implicit model with five unknown parameters: I_{ph}, I_{sd}, R_s, R_{sh}, and n.

2.2. Two-Diode Model. Due to its simplicity and accuracy, the above-mentioned single-diode model has been widely used to describe the static characteristics of the photovoltaic cell. However, the single-diode model has inherent drawbacks as it assumes that the ideality factor of the diode remains constant throughout the range of output voltage variation [29]. Currently, the closest electrical model to a photovoltaic cell is the two-diode (double exponential) model, where the cell is of course presented as an electrical current generator whose behaviour is equivalent to a current source with two diodes in parallel. The two-diode model is shown in Figure 2 [18, 52].

$$I = I_{ph} - I_{d1} - I_{d2} - I_{sh},$$

$$I_{sh} = \frac{V + R_s \times I}{R_{sh}},$$

$$\begin{aligned} I = I_{ph} &- I_{sd1}\left(\exp\left(\frac{q(V + R_s \times I)}{n_1 \times K \times T}\right) - 1\right) \\ &- I_{sd2}\left(\exp\left(\frac{q(V + R_s \times I)}{n_2 \times K \times T}\right) - 1\right) \\ &- \frac{V + R_s \times I}{R_{sh}}. \end{aligned} \tag{4}$$

The parameters of this double-diode model to be estimated are I_{ph}, I_{sd1}, I_{sd2}, R_s, R_{sh}, n_1, and n_2.

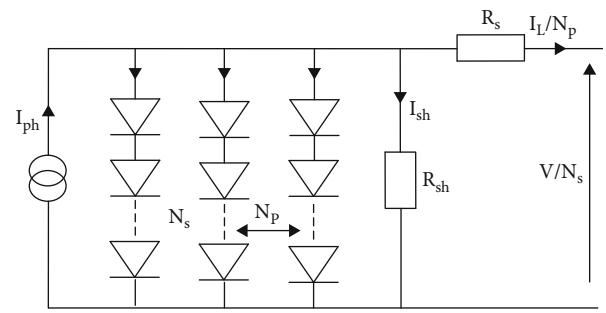

Figure 3: Equivalent model of a PV panel.

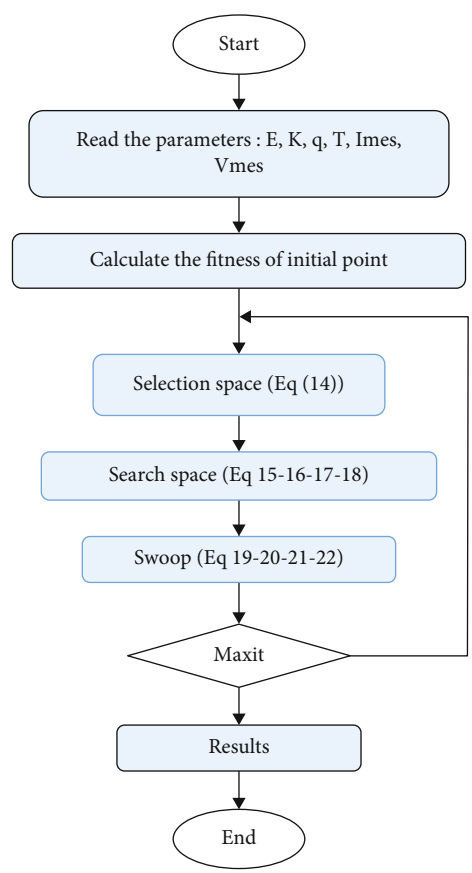

Figure 4: Flowchart of BES algorithm.

Table 1: Parameter range of different PV models.

Parameters	Single and double diode		Photowatt-PWP201		STM6-40/36		STP6-120/36	
	Lower bound	Upper bound	Lower bound	Upper bound	Lower bound	Upper bound	Lower bound	Upper bound
I_{ph} (A)	0	1	0	2	0	2	0	8
$I_{d,}I_{d1,}I_{d2}$ (μA)	0	1	0	50	0	50	0	50
R_s (Ω)	0	0.5	0	2	0	0.36	0	0.36
R_{sh} (Ω)	0	100	0	2000	0	1000	0	1500
n, n_1, n_2	1	2	1	50	1	60	1	50

Table 2: Comparison of the results obtained from single diode model R.T.C. France solar cell with other methods in the literature.

Algorithm	I_{ph} (A)	I_{sd} (μ A)	R_s (Ω)	R_{sh} (Ω)	n	RMSE
BES	**0.7607**	**0.3230**	**0.0364**	**53.7185**	**1.4812**	**9.8602*e* − 04**
ILSA [68]	0.7607	0.3229	0.0364	53.7204	1.4811	9.8602*e* − 04
GAMS [3]	0.7607	0.3230	0.0364	53.7185	1.4812	9.8602*e* − 04
ITLBO [69]	0.7607	0.3230	0.0364	53.7184	1.4812	9.8602*e* − 04
IMFO [67]	0.7607	0.3234	0.0363	53.7608	1.4813	9.8602*e* − 04
IJAYA [63]	0.7608	0.3228	0.0364	53.7595	1.4811	9.8603*e* − 04
MADE [18]	0.7607	0.3230	0.0363	53.7185	1.4811	9.8602*e* − 04
EVPS [52]	0.7607	0.3250	0.0363	53.8960	1.4821	9.8609*e* − 04
GOTLBO [64]	0.7608	0.3297	0.0363	53.3664	1.4833	9.8856*e* − 04
TLABC [20]	0.7608	0.3230	0.0364	53.7164	1.4812	9.8602*e* − 04
CLPSO [70]	0.7608	0.3430	0.0361	54.1965	1.4873	9.9633*e* − 04
TLBO [71]	0.7607	0.3294	0.0363	54.3015	1.4831	9.8733*e* − 03
TPTLBO [72]	0.7608	0.3230	0.0364	53.7185	1.4812	9.8602*e* − 04
DSCE [55]	0.7607	0.3230	0.0363	53.7185	1.4811	9.8602*e* − 04
EGBO [56]	0.7608	0.3230	0.0364	53.7185	1.4811	9.8602*e* − 04
DDSFLA [57]	0.7608	0.3191	0.036	53.3770	1.4800	9.8630*e* − 04
SFLBS [58]	0.7607	0.3230	0.0363	53.7185	1.4811	9.8602*e* − 04
LCNMSE [59]	0.7607	0.3230	0.0363	53.71	1.4811	9.8602*e* − 04
PSOCS [60]	0.7607	0.3230	0.0363	53.719	1.4812	9.8602*e* − 04
CNMSMA [61]	0.7607	0.3230	0.0363	53.7182	1.4811	9.8602*e* − 04

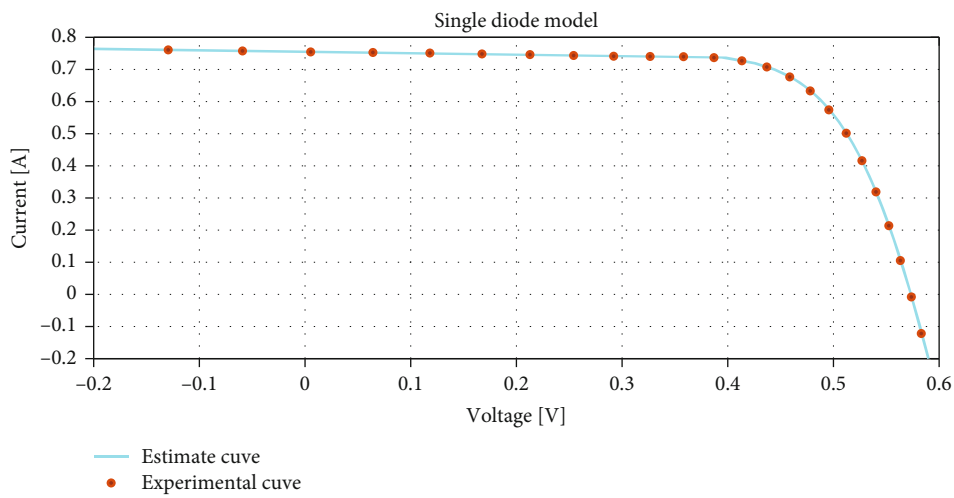

(a) I-V characteristic curve

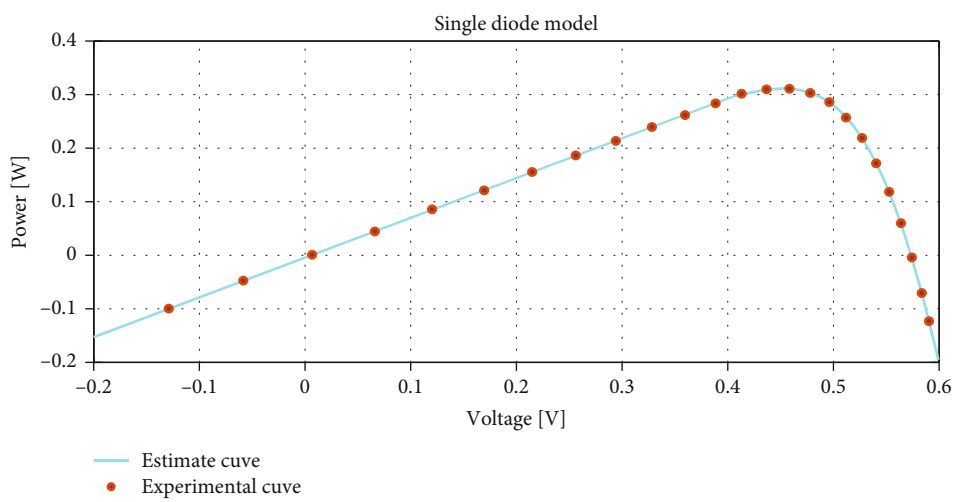

(b) P-V characteristic curve

Figure 5: Characteristics of the measured and estimated curve with one diode: (a) I-V and (b) P-V.

2.3. The PV Model. The PV module model is shown in Figure 3 [52, 63, 64].

$$I = I_{ph} \times N_p - I_{sd} \times N_p \cdot \left(\exp\left(\frac{q\left((V/N_s) + (R_s/N_p) \times I\right)}{n \times K \times T} \right) - 1 \right) - \frac{V(N_p/N_s) + R_s \times I}{R_{sh}}, \tag{5}$$

where N_p and N_s represent the number of solar cells in parallel and in series, respectively. Thus, for this PV model, five unknown parameters (I_{ph}, I_{sd}, R_s, R_{sh}, and n) have to be identified.

2.4. Objective Function. For a single-diode model, the objective function is expressed as

$$\begin{cases} f(V, I, X) = I_{ph} - I_{sd}\left(\exp\left(\frac{q(V + R_s \times I)}{n \times K \times T} \right) - 1 \right) - \frac{V + R_s \times I}{R_{sh}}, \\ X = \{I_{ph}, I_{sd}, R_s, R_{sh}, n\}. \end{cases} \tag{6}$$

For the double-diode model, the objective function is

$$\begin{cases} f(V, I, X) = I_{ph} - I_{sd1}\left(\exp\left(\frac{q(V + R_s \times I)}{n_1 \times K \times T} \right) - 1 \right) - I_{sd2}\left(\exp\left(\frac{q(V + R_s \times I)}{n_2 \times K \times T} \right) - 1 \right) - \frac{V + R_s \times I}{R_{sh}}, \\ X = \{I_{ph}, I_{sd1}, I_{sd2}, R_s, R_{sh}, n_1, n_2\}. \end{cases} \tag{7}$$

Table 3: The individual absolute error and relative error of a single-diode model obtained by BES.

Item	Test data		Simulated current		Power	
	V (V)	I (A)	I_{sim} (A)	IAE (A)	P_{sim} (W)	RE
1	−0.2057	0.7640	0.764112	0.000112	-0.157178	-0.000146
2	−0.1291	0.7620	0.762687	0.000687	-0.098463	-0.000902
3	−0.0588	0.7605	0.761379	0.000879	-0.044769	-0.001156
4	0.0057	0.7605	0.760178	0.000322	0.004333	0.000423
5	0.0646	0.7600	0.759079	0.000921	0.049037	0.001211
6	0.1185	0.7590	0.758066	0.000934	0.089831	0.001230
7	0.1678	0.7570	0.757116	0.000116	0.127044	-0.000153
8	0.2132	0.7570	0.756166	0.000834	0.161214	0.001102
9	0.2545	0.7555	0.755111	0.000389	0.192176	0.000515
10	0.2924	0.7540	0.753689	0.000311	0.220379	0.000413
11	0.3269	0.7505	0.751417	0.000917	0.245638	-0.001222
12	0.3585	0.7465	0.747383	0.000883	0.267937	-0.001183
13	0.3873	0.7385	0.740152	0.001652	0.286661	-0.002238
14	0.4137	0.7280	0.727430	0.000570	0.300938	0.000783
15	0.4373	0.7065	0.707043	0.000543	0.309190	-0.000769
16	0.4590	0.6755	0.675389	0.000111	0.310003	0.000165
17	0.4784	0.6320	0.630925	0.001075	0.301835	0.001700
18	0.4960	0.5730	0.572180	0.000820	0.283801	0.001432
19	0.5119	0.4990	0.499971	0.000971	0.255935	-0.001945
20	0.5265	0.4130	0.414157	0.001157	0.218054	-0.002802
21	0.5398	0.3165	0.318194	0.001694	0.171761	-0.005352
22	0.5521	0.2120	0.213046	0.001046	0.117623	-0.004934
23	0.5633	0.1035	0.103375	0.000125	0.058231	0.001209
24	0.5736	−0.0100	-0.007341	0.002659	-0.004211	0.265897
25	0.5833	−0.1230	-0.123850	0.000850	-0.072242	-0.006910
26	0.5900	−0.2100	-0.206601	0.003399	-0.121895	0.016186
Total IAE				0.023977		

The parameters can be estimated by minimizing the objective function RMSE(X), i.e., by searching for the solution vector x [11, 16, 29, 65, 66].

$$\mathrm{RMSE}(X) = \sqrt{\frac{1}{N}\sum_{k=1}^{N} f(V, I, X)^2}, \tag{8}$$

where X represents the parameters composed of the solution vector. V and I are the measured voltage and current, respectively. N represents the number of experiments. Hence, to estimate the parameters is equivalent to search the X in the range which minimizes the objective function.

3. Problem Formulation

The problem can be set as an optimization problem with the objective to minimize the difference between the measured and estimated current. The objective function (OF) is defined as the root mean square error (RMSE), where the error function is defined as the difference between the estimated and experimental currents. It is expressed as follows [11, 16, 29, 65, 66]:

$$\mathrm{Min}\ (\mathrm{RMSE}(X)) = \sqrt{\frac{1}{N}\sum_{k=1}^{N} (I_{k,\mathrm{mes}} - I_{k,\mathrm{ext}}(X))^2}, \tag{9}$$

where RMSE(X) is the objective function to minimize, N is the number of points measured, $I_{k,\mathrm{mes}}$ is the measured current, and $I_{k,\mathrm{ext}}(X)$ is the estimated current.

For a single-diode model, the fitness function is expressed as

$$\mathrm{Min}\ (\mathrm{RMSE}(X)) = \sqrt{\frac{1}{N}\sum_{k=1}^{N} \left(I_{k,\mathrm{mes}} - I_{\mathrm{ph}} + I_{\mathrm{sd1}} \left(\exp\left(\frac{q(V_{k,\mathrm{mes}} + R_{\mathrm{s}} \times I_{k,\mathrm{mes}})}{n_1 \times K \times T} \right) - 1 \right) + \frac{V_{k,\mathrm{mes}} + R_{\mathrm{s}} \times I_{k,\mathrm{mes}}}{R_{\mathrm{sh}}} \right)^2}, \tag{10}$$

Table 4: Statistical results for R.T.C. France PV cell single diode.

Algorithm	RMSE			
	Min	Mean	Max	Std.
BES	**9.8602*e* − 04**	**9.8602*e* − 04**	**9.8602*e* − 04**	**2.6314*e* − 13**
ITLBO	9.8602*e* − 04	9.8602*e* − 04	9.8602*e* − 4	2.19*e* − 17
IMFO	9.8602*e* − 04	9.8767*e* − 04	9.9641*e* − 04	2.1810*e* − 06
IJAYA	9.8606*e* − 04	1.0261*e* − 03	1.1223*e* − 03	4.160*e* − 05
GOTLBO	9.8602*e* − 04	1.4388*e* − 03	1.0289*e* − 03	1.01*e* − 04
CLPSO	9.9455*e* − 04	1.0507*e* − 03	1.1865*e* − 04	4.6730*e* − 05
TPTLBO	9.8602*e* − 04	9.8602*e* − 04	9.8602*e* − 04	2.28*e* − 17
MADE	9.8602*e* − 04	9.8602*e* − 04	9.8602*e* − 04	2.47*e* − 15
TLABC	9.8602*e* − 04	9.9852*e* − 04	1.2358*e* − 03	1.86*e* − 05
TLBO	9.8722*e* − 04	1.0476*e* − 04	1.0397*e* − 03	6.59*e* − 05
DSCE	9.8602*e* − 04	9.8602*e* − 04	9.8602*e* − 04	1.1320*e* − 09
EGBO	9.8602*e* − 04	9.9500*e* − 04	1.1161*e* − 04	2.62*e* − 05
DDSFLA	9.8630*e* − 04	1.0819*e* − 03	1.3056*e* − 03	8.6464*e* − 05
SFLBS	9.8602*e* − 04	9.8602*e* − 04	9.8602*e* − 04	1.4301*e* − 14
PSOCS	9.8602*e* − 04	9.8602*e* − 04	9.8603*e* − 04	1.7459*e* − 09

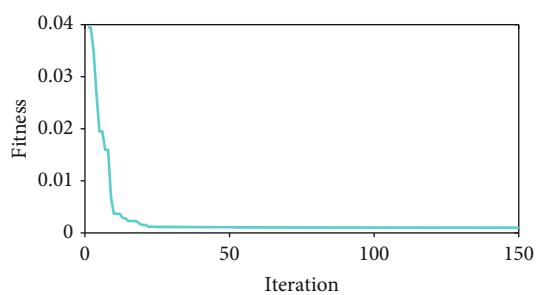

Figure 6: Convergence curve during the parameter extraction for one diode.

with $X = [I_{ph}, I_{sd}, R_s, R_{sh}, n]$ the parameters to be estimated.

For the double-diode model, the fitness function is

$$\text{Min}\,(\text{RMSE}(X)) = \sqrt{\frac{1}{N}\sum_{k=1}^{N}\left(I_{k,\text{mes}} - I_{ph} + I_{sd1}\left(\exp\left(\frac{q(V_{k,\text{mes}} + R_s \times I_{k,\text{mes}})}{n_1 \times K \times T}\right) - 1\right) + I_{sd2}\left(\exp\left(\frac{q(V_{k,\text{mes}} + R_s \times I_{k,\text{mes}})}{n_2 \times K \times T}\right) - 1\right) + \frac{V_{k,\text{mes}} + R_s \times I_{k,\text{mes}}}{R_{sh}}\right)^2}, \tag{11}$$

with $X = [I_{ph}, I_{sd1}, I_{sd2}, R_s, R_{sh}, n_1, n_2]$ the parameters to be estimated.

In this paper, the approach of bald eagle search (BES) is used for the optimization of results of equations (10) and (11).

4. Bald Eagle Search (BES) Algorithm [62]

Bald eagles are occasional predators and are at the top of the food chain only because of their size. Furthermore, bald eagles are considered scavengers that feast on any available, easy, and protein-rich food. Bald eagles are an opportunistic forager that mainly select fish (alive or dead), especially salmon, as the primary food. Bald eagles frequently hunt from perch but may also hunt while in flight. They are capable of spotting fish at enormous distances because obtaining fish from water is difficult. When they start to search for food over a water spot, these eagles set off in a specific direction and select a certain area to

Table 5: Comparison of the results obtained from the double-diode model R.T.C. France solar cell with other methods in the literature.

Algorithm	I_{ph} (A)	I_{sd1} (μA)	I_{sd2} (μA)	R_s (Ω)	R_{sh} (Ω)	n_1	n_2	Best RMSE
BES	**0.7608**	**0.2259**	**0.7493**	**0.0367**	**55.4854**	**1.4510**	**2.000**	**9.8248*e* − 4**
GAMS [3]	0.7608	0.2260	0.7594	0.0367	55.4854	1.2186	1.6247	9.8293*e* − 4
ITLBO [69]	0.7608	0.2260	0.7493	0.0367	55.4854	1.4510	2.0000	9.8248*e* − 4
IMFO [67]	0.7607	0.2350	0.6837	0.0367	55.2997	1.4537	2.0000	9.8252*e* − 4
IJAYA [63]	0.7601	0.0050	0.7509	0.0376	77.8519	1.2186	1.6247	9.8293*e* − 4
MADE [18]	0.7608	0.2246	0.7394	0.0368	55.4329	1.4505	1.9963	9.8261*e* − 4
EVPS [52]	0.7607	0.2975	0.2504	0.0363	55.8827	1.4749	1.9726	9.8510*e* − 4
GOTLBO [64]	0.7608	0.2717	0.2595	0.0366	53.6187	1.4668	1.9161	9.9544*e* − 4
CLPSO [70]	0.7606	0.2875	0.2686	0.0366	55.2895	1.9586	1.4652	9.9224*e* − 4
TLABC [20]	0.7608	0.4239	0.2401	0.0367	54.6680	1.9075	1.4567	9.8415*e* − 4
TLBO [71]	0.7610	0.2947	0.1373	0.0366	53.1210	1.4730	1.9938	1.0069*e* − 03
TPTLBO [72]	0.7608	0.7434	0.2266	0.0367	55.4831	2.0000	1.4513	9.8248*e* − 04
DSCE [55]	0.7608	0.6980	0.2318	0.0367	55.3750	1.9999	1.4553	9.8250*e* − 04
EGBO [56]	0.7608	0.225	0.749	0.0367	55.4855	1.4510	2.0000	9.8248*e* − 04
DDSFLA [57]	0.7608	0.2931	0.2271	0.0365	54.3710	1.4730	2.0000	9.8434*e* − 04
SFLBS [58]	0.7607	0.7759	0.2285	0.0367	55.5496	2.0000	1.4498	9.8249*e* − 04
LCNMSE [59]	0.7607	0.7493	0.2259	0.0367	55.4854	2.0000	1.4510	9.8248*e* − 04
PSOCS [60]	0.7607	1.0000	0.1981	0.0368	56.172	2.0000	1.4401	9.8297*e* − 04
CNMSMA [61]	0.7607	0.2259	0.7506	0.0367	55.4854	1.4510	1.9999	9.8249*e* − 04

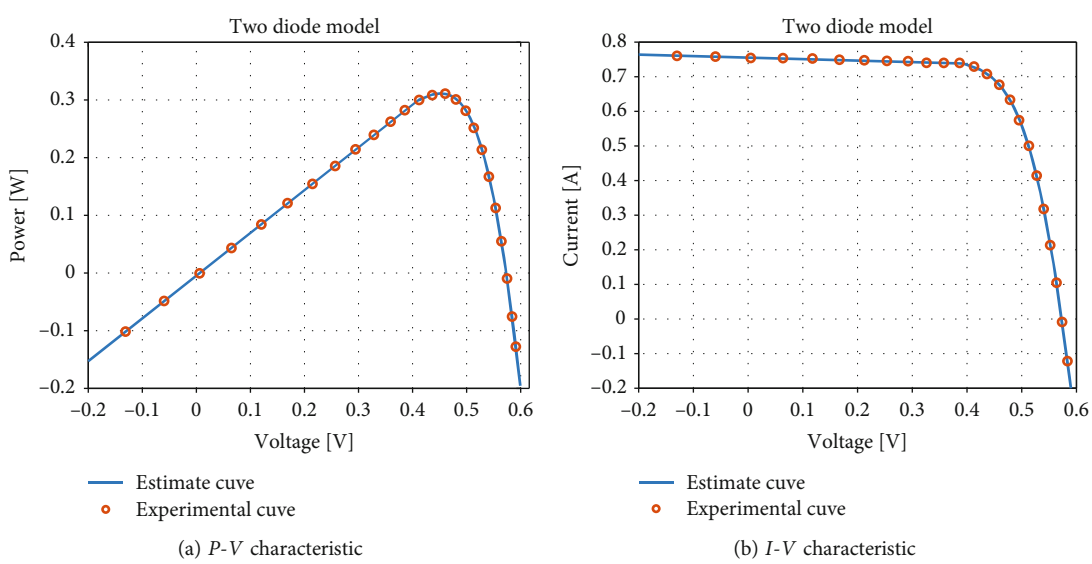

(a) P-V characteristic (b) I-V characteristic

Figure 7: Characteristics of the measured and estimated curve with two diodes: (a) P-V and (b) I-V.

Table 6: The individual absolute error and relative error of double-diode model obtained by BES.

Item	Test data		Simulated current		Power	
	V (V)	I (A)	I_{sim} (A)	IAE (A)	P_{sim} (W)	RE
1	−0.2057	0.7640	0.764003	0.000003	-0.157155	-0.000004
2	−0.1291	0.7620	0.762624	0.000624	-0.098455	-0.000818
3	−0.0588	0.7605	0.761357	0.000857	-0.044768	-0.001127
4	0.0057	0.7605	0.760193	0.000307	0.004333	0.000403
5	0.0646	0.7600	0.759127	0.000873	0.049040	0.001148
6	0.1185	0.7590	0.758141	0.000859	0.089840	0.001132
7	0.1678	0.7570	0.757208	0.000208	0.127060	-0.000275
8	0.2132	0.7570	0.756263	0.000737	0.161235	0.000973
9	0.2545	0.7555	0.755197	0.000303	0.192198	0.000400
10	0.2924	0.7540	0.753744	0.000256	0.220395	0.000340
11	0.3269	0.7505	0.751423	0.000923	0.245640	-0.001230
12	0.3585	0.7465	0.747332	0.000832	0.267919	-0.001114
13	0.3873	0.7385	0.740054	0.001554	0.286623	-0.002104
14	0.4137	0.7280	0.727313	0.000687	0.300889	0.000943
15	0.4373	0.7065	0.706955	0.000455	0.309151	-0.000644
16	0.4590	0.6755	0.675376	0.000124	0.309997	0.000184
17	0.4784	0.6320	0.631010	0.000990	0.301875	0.001567
18	0.4960	0.5730	0.572351	0.000649	0.283886	0.001132
19	0.5119	0.4990	0.500188	0.001188	0.256046	-0.002381
20	0.5265	0.4130	0.414353	0.001353	0.218157	-0.003277
21	0.5398	0.3165	0.318305	0.001805	0.171821	-0.005702
22	0.5521	0.2120	0.213015	0.001015	0.117605	-0.004787
23	0.5633	0.1035	0.103172	0.000328	0.058117	0.003166
24	0.5736	−0.0100	-0.007691	0.002309	-0.004412	0.230909
25	0.5833	−0.1230	-0.124367	0.001367	-0.072543	-0.011111
26	0.5900	−0.2100	-0.207164	0.002836	-0.122226	0.013507
Total IAE				0.023441		

Table 7: Statistical results for R.T.C. France PV cell two diodes.

Algorithm	RMSE			
	Min	Mean	Max	Std.
BES	**9.8248e − 04**	**9.9518e − 04**	**1.1881e − 03**	**4.6013e − 05**
ITLBO	9.8248e − 04	9.8812e − 04	9.8497e − 04	1.54e − 06
IMFO	9.8252e − 04	9.9737e − 04	1.1409e − 03	3.2939e − 05
IJAYA	9.8380e − 04	1.0240e − 03	1.3507e − 03	8.5647e − 05
GOTLBO	9.8407e − 04	1.4380e − 03	1.0453e − 03	1.01e − 04
CLPSO	9.9224e − 04	1.0522e − 03	1.1462e − 03	4.3141e − 05
TPTLBO	9.8248e − 04	9.8602e − 04	9.8363e − 04	9.31e − 07
MADE	9.8261e − 04	9.8608e − 04	9.8786e − 04	8.02e − 05
TLABC	9.8415e − 04	1.0555e − 03	1.5048e − 03	1.54e − 06
TLBO	1.0069e − 03	1.1598e − 03	1.5206e − 03	1.56e − 04
EGBO	9.8248e − 04	9.8484e − 04	9.8681e − 04	1.66e − 04
DDSFLA	9.8434e − 04	1.1071e − 03	1.4225e − 03	1.3014e − 04
SFLBS	9.8249e − 04	9.8541e − 04	9.8787e − 04	1.7882e − 06
PSCOS	9.8297e − 04	1.0286e − 03	1.4133e − 03	9.9217e − 05

begin the search. Accordingly, finding the search space is achieved by self-searching and tracking other birds with the concentration of fish (dead or alive).

The proposed BES algorithm mimics the behaviour of bald eagles during hunting to justify the consequences of each hunting step. This algorithm is divided into three parts, namely, search space selection, search in the selected search space, and swooping.

4.1. Selection Stage. In the selection stage, bald eagles identify and select the best area (in terms of amount of food) within the selected search space where they can hunt for prey. Equation (12) presents this behaviour mathematically.

$$P_{i,\text{new}} = P_{\text{best}} + \alpha * (P_{\text{mean}} - P_i) * r, \tag{12}$$

where α is the position change control parameter that takes a value between 1.5 and 2 and r is a random number that takes a value between 0 and 1; $P_{i,\text{new}}$ and P_i are updated position and old position, respectively, at time i. In the selection step, the bald eagles select an area based on the information available from the previous step. The eagles randomly select another search area that differs from the previous search area but is located nearby. P_{best} denotes the search area that is currently selected by the bald eagles based on the best position identified in their previous search. The eagles randomly search all points near the previously selected search space. Meanwhile, P_{mean} indicates that these eagles have used all the information from the previous points.

4.2. Search Stage. In the search stage, bald eagles search for prey within the selected search space and move in different directions within a spiral space to accelerate their search.

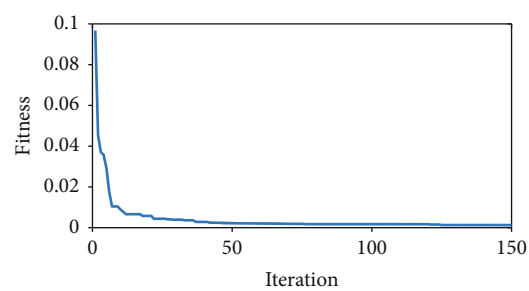

Figure 8: Convergence curve during the parameter extraction for the two-diode models.

The best position for the swoop is mathematically expressed in

$$P_{i,\text{new}} = P_i + y(i) * (P_i - P_{i+1}) + x(i) * (P_i - P_{\text{mean}}), \tag{13}$$

$$x(i) = \frac{xr(i)}{\max(|xr|)}, \tag{14}$$

$$y(i) = \frac{yr(i)}{\max(|yr|)}, \tag{15}$$

$$xr(i) = r(i) * \sin(\theta(i)), \tag{16}$$

$$yr(i) = r(i) * \cos(\theta(i)), \tag{17}$$

$$\theta(i) = a * \pi * \text{rand}, \tag{18}$$

$$r(i) = \theta(i) + R * \text{rand}, \tag{19}$$

where a is a parameter that takes a value between 5 and 10 for determining the corner point search in the central point and R takes a value between 0.5 and 2 for determining the number of search cycles.

Table 8: Comparison of the results obtained from Photowatt-PWP201 model with other methods in the literature.

Algorithm	I_{ph} (A)	I_{sd} (μ A)	R_s (Ω)	R_{sh} (Ω)	n	RMSE
BES	**1.0305**	**3.4823**	**1.2013**	**981.9824**	**48.6428**	**2.42507e – 03**
GAMS [3]	1.0320	3.2681	1.2062	828.2928	1.3445	2.4426e – 03
ITLBO [69]	1.0305	3.4823	1.2013	981.9823	48.6428	2.4251e – 03
IMFO [67]	1.0305	3.4783	1.2013	980.4672	48.6385	2.4251e – 03
IJAYA [63]	1.0302	3.4703	1.2011	984.8760	48.6482	2.4251e – 03
MADE [18]	1.0305	3.4823	1.2013	981.9823	48.6428	2.4251e – 03
EVPS [52]	1.0318	3.2679	1.2066	845.759	1.3445	2.4267e – 03
GOTLBO [64]	1.0305	3.4991	1.2008	989.6889	48.6611	2.4251e – 03
TLABC [20]	1.0306	3.4715	1.2017	972.9357	48.6313	2.4251e – 03
TLBO [71]	1.0305	3.4872	1.2011	984.8760	48.6482	2.4251e – 03
CLPSO [70]	1.0304	3.6131	1.1978	1017.0	48.7847	2.4280e – 03
TPTLBO [72]	1.0305	3.4823	1.2013	981.9822	48.6428	2.4251e – 03
EGBO [56]	1.0305	3.48	1.2013	981.9822	48.6428	2.4151e – 03
DDSFLA [57]	1.0306	3.4473	1.2023	971.2500	48.6040	2.4252e – 03
SFLBS [58]	1.0305	3.4822	1.2012	981.9804	48.6428	2.4251e – 03
LCNMSE [59]	1.0315	3.4822	1.2013	981.9741	48.6428	2.4251e – 03
PSOCS [60]	1.0305	3.4823	1.2013	981.98	48.643	2.4251e – 03

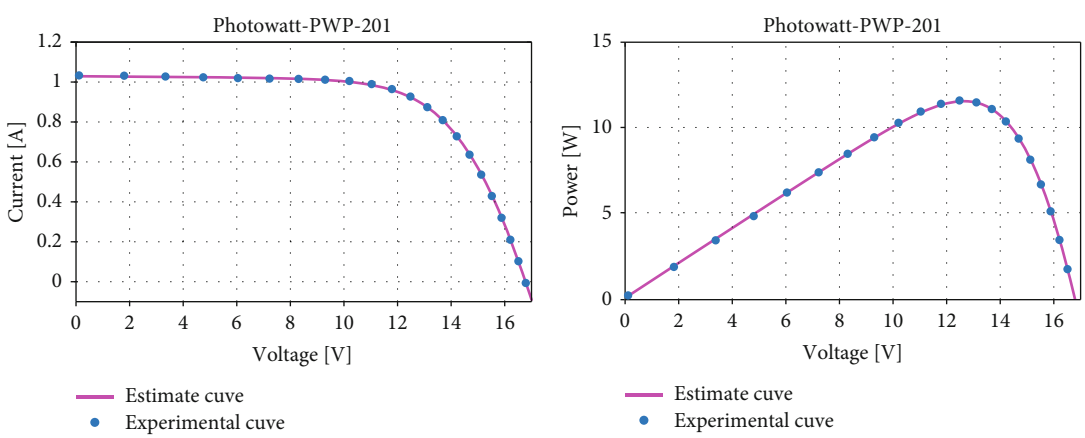

(a) I-V characteristic curve (b) P-V characteristic curve

Figure 9: Characteristics of the measured and estimated curve with one diode: (a) I-V and (b) P-V.

Table 9: The individual absolute error and relative error of Photowatt-PWP201 obtained by BES.

Item	Test data		Simulated current		Power	
	V (V)	I (A)	I_{sim} (A)	IAE (A)	P_{sim} (W)	RE
1	0.1248	1.0315	1.029105	0.002395	0.128432	0.002322
2	1.8093	1.0300	1.027367	0.002633	1.858815	0.002557
3	3.3511	1.0260	1.025728	0.000272	3.437315	0.000266
4	4.7622	1.0220	1.024093	0.002093	4.876936	-0.002048
5	6.0538	1.0180	1.022278	0.004278	6.188666	-0.004202
6	7.2364	1.0155	1.019918	0.004418	7.380532	-0.004350
7	8.3189	1.0140	1.016352	0.002352	8.454931	-0.002320
8	9.3097	1.0100	1.010490	0.000490	9.407354	-0.000485
9	10.2163	1.0035	1.000631	0.002869	10.222748	0.002859
10	11.0449	0.9880	0.984567	0.003433	10.874439	0.003475
11	11.8018	0.9630	0.959567	0.003433	11.324616	0.003565
12	12.4929	0.9255	0.922926	0.002574	11.530023	0.002781
13	13.1231	0.8725	0.872748	0.000248	11.453153	-0.000284
14	13.6983	0.8075	0.807504	0.000004	11.061434	-0.000005
15	14.2221	0.7265	0.728669	0.002169	10.363202	-0.002985
16	14.6995	0.6345	0.637592	0.003092	9.372288	-0.004874
17	15.1346	0.5345	0.536806	0.002306	8.124337	-0.004313
18	15.5311	0.4275	0.430253	0.002753	6.682303	-0.006440
19	15.8929	0.3185	0.319674	0.001174	5.080544	-0.003686
20	16.2229	0.2085	0.208450	0.000050	3.381663	0.000240
21	16.5241	0.1010	0.097391	0.003609	1.609294	0.035736
22	16.7987	−0.0080	-0.006947	0.001053	-0.116694	0.131670
23	17.0499	−0.1110	-0.109404	0.001596	-1.865323	0.014380
24	17.2793	−0.2090	-0.207566	0.001434	-3.586589	0.006863
25	17.4885	−0.3030	-0.299042	0.003958	-5.229796	0.013063
Total IAE				0.054687		

Table 10: The statistical results for Photowatt-PWP201.

Algorithm	RMSE			
	Min	Mean	Max	Std.
BES	**2.42507*e* − 3**	**2.42507*e* − 3**	**2.42507*e* − 3**	**2.4532*e* − 17**
ITLBO	2.4251*e* − 03	2.4251*e* − 03	2.4251*e* − 03	1.27*e* − 17
IMFO	2.4251*e* − 03	2.4294*e* − 03	2.5005*e* − 03	1.3831*e* − 05
IJAYA	2.4251*e* − 03	2.4393*e* − 03	2.4289*e* − 03	3.78*e* − 06
GOTLBO	2.4251*e* − 03	2.4852*e* − 03	2.4419 *e* − 03	1.38*e* − 05
CLPSO	2.4280*e* − 03	2.4549*e* − 03	2.5432*e* − 03	2.5809*e* − 05
TPTLBO	2.4251*e* − 03	2.4251*e* − 03	2.4251*e* − 03	1.20*e* − 17
MADE	2.4250*e* − 03	2.4251*e* − 03	2.4251*e* − 03	1.96*e* − 16
TLABC	2.4251*e* − 03	2.4265*e* − 03	2.4458*e* − 03	4.00*e* − 06
TLBO	2.4251*e* − 03	2.4383*e* − 03	2.5475*e* − 03	2.43*e* − 05
EGBO	2.4251*e* − 03	2.4251*e* − 03	2.4251*e* − 03	2.38*e* − 17
DDSFLA	2.4252*e* − 03	2.4974*e* − 03	2.9281*e* − 03	1.1000*e* − 04
SFLBS	2.4251*e* − 03	2.4251*e* − 03	2.4251*e* − 03	3.9417*e* − 17
PSOCS	2.4251*e* − 03	2.4252*e* − 03	2.4282*e* − 03	5.9113*e* − 07

This algorithm uses the polar graph property to mathematically represent this movement. This property also allows the BES algorithm to discover new spaces and increase diversification by multiplying the difference between the current point and the next point with the polar point in the y-axis and adding the difference between the current point and the center point with the polar point in the x-axis. We use the average solution in the search point because all search points move towards the centre point. All points in the polar plot take a value between -1 and 1, and we use a special equation for the shape of the spiral (20–22).

4.3. Swooping Stage. In the swooping stage, bald eagles swing from the best position in the search space to their target prey. All points also move towards the best point. Equation (14) mathematically illustrates this behaviour.

$$\begin{aligned} P_{i,\text{new}} &= \text{rand} * P_{\text{best}} + x1(i) * (P_i - c1 * P_{\text{mean}}) \\ &\quad + y1(i) * (P_i - c2 * P_{\text{best}}), \\ x1(i) &= \frac{xr(i)}{\max(|xr|)}, \\ y1(i) &= \frac{yr(i)}{\max(|yr|)}, \\ xr(i) &= r(i) * \sinh(\theta(i)), \\ yr(i) &= r(i) * \cosh(\theta(i)), \\ \theta(i) &= a * \pi * \text{rand}, \\ r(i) &= \theta(i), \end{aligned} \tag{20}$$

where $c1, c2 \in [1, 2]$.

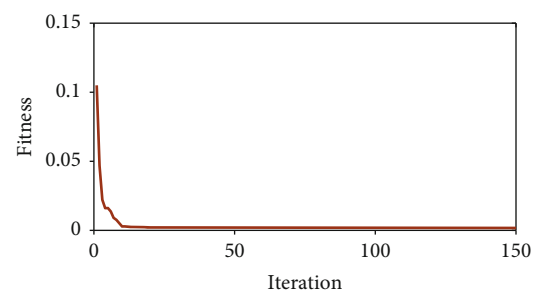

Figure 10: Convergence curve during the parameter extraction for the two-diode models.

4.4. Complete BES Algorithm. The previous steps have presented the main components of BES, which include the selection, search, and swooping steps. To describe the remaining operations and facilitate the implementation of BES, the flowchart algorithm is described in Figure 4:

5. Simulation Results and Analysis

The BES algorithm is applied to extract the SDM, DDM, and PV module parameters. To examine in more detail the accuracy of the data obtained by the BES method for the optimized parameters, the current was calculated from the values estimated on the basis of the different models and compared with that obtained from the experimental measurements. The error in the measured values for each of the models was evaluated by IAE (individual absolute error) and RE (relative error), calculated as shown in equations (21) and (22), respectively.

$$\text{IAE} = |I_{\text{measured}} - I_{\text{estimated}}|, \tag{21}$$

$$\text{RE} = \frac{I_{\text{measured}} - I_{\text{estimated}}}{I_{\text{measured}}}. \tag{22}$$

Table 11: Comparison of the results obtained from Solar STM6-40/36 PV model with other methods in the literature.

Algorithm	I_{ph} (A)	I_{sd} (μA)	R_s (Ω)	R_{sh} (Ω)	n	RMSE
BES	**1.6639**	**1.7387**	**0.0043**	**15.9283**	**1.5203**	**1.7298*e* – 03**
ITLBO [69]	1.6639	1.7387	0.0043	15.9283	1.5203	1.7298*e* – 03
IJAYA [63]	1.6637	1.8353	0.0040	15.9449	1.5263	1.7548*e* – 03
MADE [18]	1.6639	1.1387	0.0043	15.9283	1.5203	1.7298*e* – 03
GOTLBO [64]	1.6639	1.7387	0.0043	15.9283	1.5203	1.7298*e* – 03
TPTLBO [72]	1.6639	1.7387	0.0043	15.9283	1.5203	1.7298*e* – 03
TLABC [20]	1.6639	1.7387	0.0043	15.9283	1.5203	1.7298*e* – 03
TLBO [71]	1.6638	1.7307	0.0043	15.9955	1.5198	1.7305*e* – 03
EGBO [56]	1.6639	1.73	0.0043	15.9283	1.5203	1.7298*e* – 03

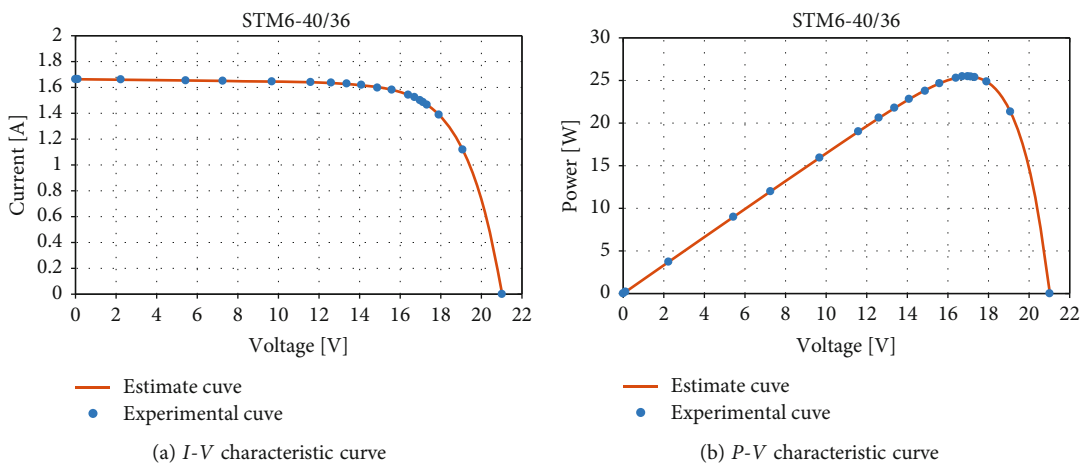

(a) I-V characteristic curve (b) P-V characteristic curve

Figure 11: Characteristics of the measured and estimated curve Schutten Solar STM6-40/36 PV model: (a) I-V and (b) P-V.

The lower and upper bounds are expressed in Table 1 [18, 63, 67].

5.1. Case Study 1: Single-Diode Model. In this case study, the BES optimization algorithm is used to extract the parameters of the two proposed models of the R.T.C. France solar cell. The measured data of the characteristic curves (I-V) of the R.T.C. France solar cell are reported in [63, 67]. Table 2 includes the results of the parameters estimated based on BES and those estimated based on other optimization techniques such as ILSA [68], GAMS [3], ITLBO [69], IMFO [67], IJAYA [63], MADE [18], EVPS [52], GOTLBO [64], DDSFLA [57], EGBO [56], and CLPSO [70]. From Table 2, it can be seen that for the SDM, the application of the proposed BES algorithm results in the minimum RMSE value which is equal to **9.8602*e* – 04**.

From Figure 5, it can be clearly seen that the I-V and P-V curves of the simulated data found by BES are very compatible with the experimental data.

From Table 3, it is evident that all IAE values are lower than 3.399*e* – 03 and the RE values are between −6.91*e* – 03 and 2.65897*e* – 01, demonstrating the high efficiency identified by BES for the single-diode model.

Table 4 and Figure 6 show the statistical results and the convergence curve, respectively. From Table 4, it can be seen that BES obtains the best minimum value of RMSE.

5.2. Case Study 2: Two-Diode Model. Table 5 lists the results obtained from the application of the BES technique to extract the DDM parameters of the R.T.C. France solar cell. To validate the applied technique, the table also presents the results from the application of other techniques of GAMS [3], ITLBO [69], IMFO [67], IJAYA [63], MADE [18], EVPS [52], GOTLBO [64], and CLPSO [70]. The table shows that the BES optimization technique applied gives the best results with the minimum objective function of RMSE being **0.000982484851801148**.

From Figure 7, it can be clearly seen that the I-V and P-V curves of the simulated data found by BES are very compatible with the experimental data.

From Table 6, it is evident that all IAE values are lower than 2.836*e* – 03 and the RE values are between −1.1111*e* – 02 and 2.3090*e* – 01, demonstrating the high efficiency identified by BES for the two-diode model.

Table 7 and Figure 8 show the statistical results and the convergence curve, respectively. From Table 7, it can be seen that BES obtains the best minimum value of RMSE.

Table 12: The individual absolute error and relative error of Schutten Solar STM6-40/36 PV model obtained by BES.

Item	Test data		Simulated current		Power	
	V (V)	I (A)	I_{sim} (A)	IAE (A)	P_{sim} (W)	RE
1	0.000	1.663	1.663453	0.000453	0.000000	-0.000273
2	0.118	1.663	1.663247	0.000247	0.196263	-0.000149
3	2.237	1.661	1.659546	0.001454	3.712404	0.000875
4	5.434	1.653	1.653910	0.000910	8.987346	-0.000550
5	7.26	1.65	1.650561	0.000561	11.983074	-0.000340
6	9.68	1.645	1.645426	0.000426	15.927728	-0.000259
7	11.59	1.64	1.639232	0.000768	18.998696	0.000468
8	12.6	1.636	1.633714	0.002286	20.584802	0.001397
9	13.37	1.629	1.627293	0.001707	21.756902	0.001048
10	14.09	1.619	1.618328	0.000672	22.802247	0.000415
11	14.88	1.597	1.603120	0.006120	23.854427	-0.003832
12	15.59	1.581	1.581642	0.000642	24.657796	-0.000406
13	16.4	1.542	1.542430	0.000430	25.295849	-0.000279
14	16.71	1.524	1.521318	0.002682	25.421217	0.001760
15	16.98	1.5	1.499347	0.000653	25.458914	0.000435
16	17.13	1.485	1.485445	0.000445	25.445677	-0.000300
17	17.32	1.465	1.465849	0.000849	25.388510	-0.000580
18	17.91	1.388	1.387887	0.000113	24.857056	0.000081
19	19.08	1.118	1.119065	0.001065	21.351757	-0.000952
20	22.02	0	0.002386	0.002386	0.050143	—
Total IAE				0.02486996		

Table 13: The statistical results for Photowatt STM6-40/36.

Algorithm	RMSE			
	Min	Mean	Max	Std.
BES	**1.7298*e* − 03**	**1.7298*e* − 03**	**1.7298*e* − 03**	**5.6525*e* − 18**
ITLBO	1.7298*e* − 03	1.7298*e* − 03	1.7298*e* − 03	7.13*e* − 03
IJAYA	17548*e* − 03	2.5223*e* − 03	1.9305*e* − 03	1.91*e* − 04
GOTLBO	1.7298*e* − 03	1.1244*e* − 03	4.2347*e* − 03	6.41*e* − 02
TPTLBO	1.7298*e* − 03	1.7298*e* − 03	1.7298*e* − 03	4.96*e* − 18
MADE	1.7298*e* − 03	1.7298*e* − 03	1.7298*e* − 03	8.49*e* − 14
TLABC	1.7298*e* − 03	2.1827*e* − 03	6.5053*e* − 03	9.22*e* − 04
TLBO	1.7305*e* − 03	4.3487*e* − 03	2.0593*e* − 02	3.45*e* − 03
EGBO	1.7298*e* − 03	1.7298*e* − 03	1.7298*e* − 03	8.22*e* − 18

5.3. Case Study 3: Photowatt-PWP201 PV Module. To further validate the BES technique and show its effectiveness in estimating the optimal parameters of different models, we used this algorithm on the Photowatt-PWP201 PV module, which consists of 36 silicon cells connected in series under operating conditions of 1000 W/m^2 of solar irradiation and a cell temperature of 45°C. The results obtained were compared with those reported in the literature based on other techniques.

The results have been listed in Table 8. This table also presents a comparison with the results of other techniques from

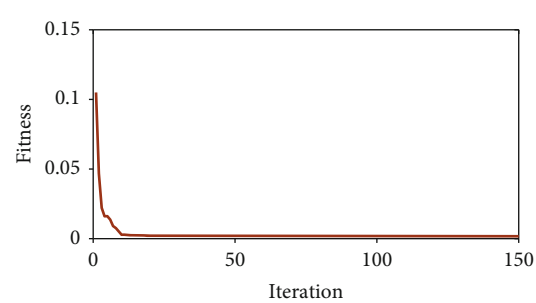

Figure 12: Convergence curve during the parameter extraction for Solar STM6-40/36 PV model.

Table 14: Comparison of the results obtained from Solar STP6-120/36 PV model with other methods in the literature.

Algorithm	I_{ph} (A)	I_{sd} (μ A)	R_s (Ω)	R_sh (Ω)	n	RMSE
BES	7.4716	2.3218	0.0046	23.0265	1.2596	**1.6782*e* − 03**
ITLBO [69]	7.4725	2.3350	0.0046	22.2199	1.2601	1.6601*e* − 02
IJAYA [63]	7.4672	2.2536	0.0046	27.5925	1.2571	1.6731*e* − 02
MADE [18]	7.4725	2.3350	0.0046	22.2199	1.2601	1.6601*e* − 02
GOTLBO [64]	7.4725	2.3350	0.0046	22.2199	1.2601	1.6601*e* − 02
TPTLBO [72]	7.4757	3.0100	0.0046	22.2199	1.2601	3.0343*e* − 01
TLABC [20]	7.4725	2.3349	0.0046	22.2117	1.2601	1.6601*e* − 02
TLBO [71]	7.4782	1.9194	0.0047	13.2688	1.2440	1.6892*e* − 02
EGBO [56]	7.4725	2.33	0.0046	22.2199	1.2601	1.6601*e* − 02

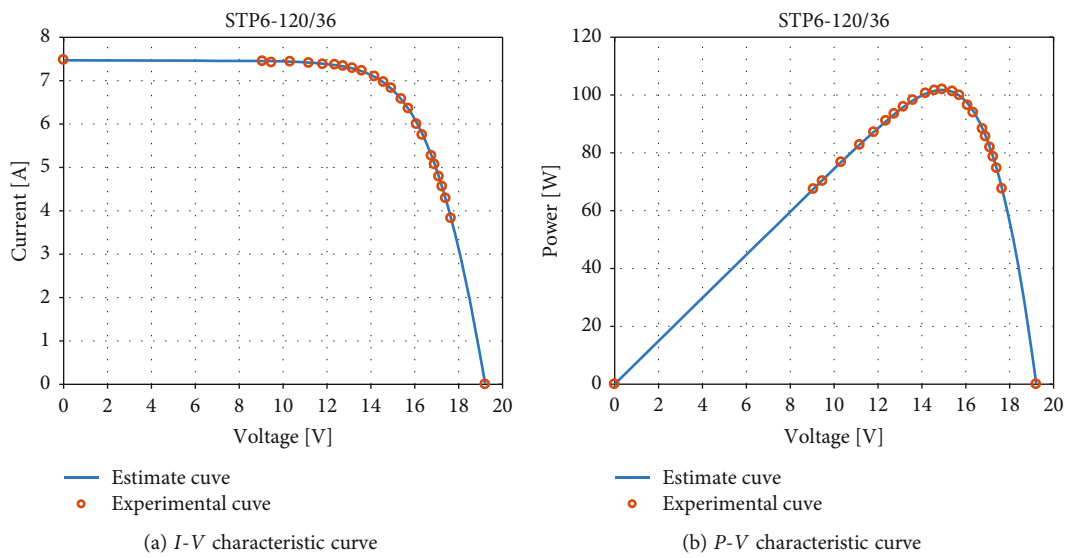

(a) I-V characteristic curve (b) P-V characteristic curve

Figure 13: Characteristics of the measured and estimated curve SPT6-120/36: (a) I-V and (b) P-V.

the literature ITLBO [69], IMFO [67], IJAYA [63], and MADE [18]. The comparison validated the effectiveness of BES compared to other techniques. The RMSE based on BES application to extract the parameters of PV model is equal to 0.00242507 which is better. From Figure 9, it can be clearly seen that the I-V and P-V curves of the simulated data found by BES are very compatible with the experimental data.

From Table 9, it is evident that all IAE values are lower than 4.418e − 03 and the RE values are between −6.44e − 03 and 1.3167e − 01, demonstrating the high efficiency identified by BES for the PV model.

Table 10 and Figure 10 show the statistical results and the convergence curve, respectively. From Table 10, it can be seen BES obtains the best minimum value of RMSE.

5.4. Case Study 4: Schutten Solar STM6-40/36 Monocrystalline PV Module. Here, we use the BES algorithm to extract the parameters of the Schutten Solar STM6-40/36 PV module. It contains 36 polycrystalline cells (size 156 mm × 156 mm) connected in series. The data set contains 20 data points measured at $T = 51°C$ [66]. For the STM6-40/36 PV module model, Table 11 shows the results of the parameters obtained from ITLBO, IJAYA, GOTLBO, TPTLBO …. From the results, it can be seen that the BES provides a better RMSE: **0.00172981370994066**.

In addition, to confirm the accuracy of the extracted parameters, Figure 11 shows the I-V and P-V curves. It is evident that the simulated data from the BES match well with the measured data in the voltage range for both I-V and P-V curves.

In addition, the IAE and RE (relative error) are given in Table 12. The IAE describes the error between the extracted parameter and the measured data. In other words, the extracted parameters are better when the IAE is small. According to Table 12, the sum of the IAE is less than 2.50 E − 02, which indicates that the measured and extracted data coincide well.

To further prove the reliability of the BES, the statistical results containing the minimum (Min), maximum (Max), mean value (Mean), and standard deviation (Std.) are analyzed. Table 13 shows the statistical results, and Figure 12 shows the convergence curve of Photowatt STM6-40/36.

Table 15: The individual absolute error and relative error of Solar STP6-120/36 PV model obtained by BES.

Item	Test data		Simulated current		Power	
	V (V)	I (A)	I_{sim} (A)	IAE (A)	P_{sim} (W)	RE
1	0	7.48	7.470103	0.009897	91.007384	0.001323
2	9.06	7.45	7.452081	0.002081	93.400729	-0.000279
3	9.47	7.42	7.448954	0.028954	95.858207	-0.003902
4	10.32	7.44	7.438716	0.001284	98.086936	0.000173
5	11.17	7.41	7.420020	0.010020	100.437238	-0.001352
6	11.81	7.38	7.395783	0.015783	101.453230	-0.002139
7	12.36	7.37	7.363057	0.006943	101.740893	0.000942
8	12.74	7.34	7.331297	0.008703	101.079430	0.001186
9	13.16	7.29	7.284058	0.005942	99.739277	0.000815
10	13.59	7.23	7.217582	0.012418	97.226742	0.001718
11	14.17	7.1	7.088020	0.011980	94.528700	0.001687
12	14.58	6.97	6.958383	0.011617	88.460738	0.001667
13	14.93	6.83	6.814527	0.015473	86.006230	0.002265
14	15.39	6.58	6.567864	0.012136	81.881540	0.001844
15	15.71	6.36	6.348776	0.011224	78.409965	0.001765
16	16.08	6	6.046439	0.046439	74.377396	-0.007740
17	16.34	5.75	5.785110	0.035110	67.754636	-0.006106
18	16.76	5.27	5.278087	0.008087	0.274440	-0.001535
19	16.9	5.07	5.089126	0.019126	91.007384	-0.003772
20	17.1	4.79	4.788394	0.001606	93.400729	0.000335
21	17.25	4.56	4.545505	0.014495	95.858207	0.003179
22	17.41	4.29	4.272108	0.017892	98.086936	0.004171
23	17.65	3.83	3.838790	0.008790	100.437238	-0.002295
24	19.21	0	0.014286	0.014286	101.453230	—
Total IAE				0.330286		

Table 16: The statistical results for Photowatt STP6-120/36 obtained by BES.

Algorithm	RMSE			
	Min	Mean	Max	Std.
BES	**1.6782*e* − 02**	**1.69034*e* − 02**	**1.7223*e* − 02**	**1.1219*e* − 04**
ITLBO	1.6601*e* − 02	1.6601*e* − 02	1.6601*e* − 02	7.22*e* − 17
IJAYA	1.6731*e* − 02	1.6891*e* − 02	1.7304*e* − 02	1.12*e* − 04
GOTLBO	1.6601*e* − 02	2.9588*e* − 02	1.8099*e* − 01	3.05*e* − 02
MADE	1.6601*e* − 02	1.6601*e* − 02	1.6601*e* − 02	1.69*e* − 15
TLABC	1.6601*e* − 02	1.6963*e* − 02	2.1497*e* − 02	9.47*e* − 04
TLBO	1.6892*e* − 02	3.6690*e* − 02	2.1604*e* − 02	3.51*e* − 02
EGBO	1.6601*e* − 02	1.6601*e* − 04	1.6601*e* − 02	1.47*e* − 16

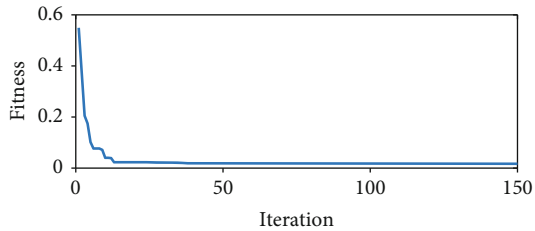

Figure 14: Convergence curve during the parameter extraction for Solar STP6-120/36 PV model.

5.5. Case Study 5: STP6-120/36 Module. The polycrystalline STP6-120/36 has 36 cells connected in series and is measured under 1000 W/m^2 at 55°C. The current-voltage data was obtained from [72]. The results have been listed in Table 14. This table also presents a comparison with the results of other techniques from the literature ITLBO [69], IMFO [67], IJAYA [63], TLABC [20], GOTLBO [64], and MADE [18]. The comparison validated the effectiveness of BES compared to other techniques. The RMSE based on BES application to extract the parameters of PV model equals 0.0167828544285882. From Figure 13, it can be clearly seen that the I-V and P-V curves of the simulated data found by BES are very compatible with the experimental data.

In addition, the IAE and RE (relative error) are given in Table 15. The IAE describes the error between the extracted parameter and the measured data. In other words, the extracted parameters are better when the IAE is small. According to Table 15, the sum of the IAE is less than 4.64 $E-02$, which indicates that the measured and extracted data coincide well.

Table 16 and Figure 14 show the statistical results and the convergence curve, respectively.

6. Conclusion

In this paper, we have presented a new and very recent algorithm based on the metaheuristic technique, called the bald eagle search (BES) algorithm to extract the best values of cell and panel parameters. To demonstrate the performance of the algorithm, many cases were implemented using the single-diode, double-diode, and PV panel models. The current-voltage and power-voltage characteristics of the measured and estimated data show the good accuracy of the proposed method. Simulation result after 20 tests and comparisons with other methods show the accuracy and validity of the method for extracting the parameters of a PV cell and module. It has the advantage of producing stable results of each test result and converging rapidly (in less than 50 iterations). The method is verified using practical data from various manufacturers. Its accuracy is confirmed by comparing its RMSE with many metaheuristic methods. In all considered scenarios, a high level of accuracy is obtained. Therefore, the excellent correspondence of the simulated I-V and P-V curves with the measured characteristics confirms the accuracy of the BES and its applicability to parameter estimation and for solving the optimization problems of other power systems.

Conflicts of Interest

The authors declare that they have no conflicts of interest.

References

[1] S. R. Madeti and S. N. Singh, "Monitoring system for photovoltaic plants: a review," *Renewable and Sustainable Energy Reviews*, vol. 67, pp. 1180–1207, 2017.

[2] Tshwane University of Technology, Department of Electrical Engineering, Pretoria, 0001, South Africa, M. U. Olanipekun, J. L. Munda, H. W. G. Chen, and A. S. Kumar, "Estimation of maximum power generated from CIGS photovoltaic modules under non-uniform conditions," *International Journal of Smart Grid and Clean Energy*, vol. 3, no. 3, pp. 318–324, 2014.

[3] P. J. Gnetchejo, S. Ndjakomo Essiane, P. Ele, R. Wamkeue, D. Mbadjoun Wapet, and S. Perabi Ngoffe, "Important notes on parameter estimation of solar photovoltaic cell," *Energy Conversion and Management*, vol. 197, article 111870, 2019.

[4] B. Jacob, K. Balasubramanian, S. Babu T, S. M. Azharuddin, and N. Rajasekar, "Solar PV modelling and parameter extraction using artificial immune system," *Energy Procedia*, vol. 75, pp. 331–336, 2015.

[5] D. Kler, Y. Goswami, K. P. S. Rana, and V. Kumar, "A novel approach to parameter estimation of photovoltaic systems using hybridized optimizer," *Energy Conversion and Management*, vol. 187, pp. 486–511, 2019.

[6] A. Jain, "Exact analytical solutions of the parameters of real solar cells using Lambert W-function," *Solar Energy Materials & Solar Cells*, vol. 81, no. 2, pp. 269–277, 2004.

[7] S. Lun, C. Du, T. Guo, S. Wang, J. Sang, and J. Li, "A new explicit I-V model of a solar cell based on Taylor 's series expansion," *Solar Energy*, vol. 94, pp. 221–232, 2013.

[8] S. Lun, T. Guo, and C. Du, "A new explicit I-V model of a silicon solar cell based on Chebyshev Polynomials," *Solar Energy*, vol. 119, pp. 179–194, 2015.

[9] J. Ma, T. Guo, and S. Lun, "An new explicit I–V model based on Chebyshev polynomials for two-diode model of photovoltaic modules," in *Proceedings of 2014 IEEE International Conference on Service Operations and Logistics, and Informatics*, pp. 362–367, Qingdao, China, 2014.

[10] P. J. Gnetchejo, S. Ndjakomo Essiane, A. Dadjé, and P. Ele, "A combination of Newton-Raphson method and heuristics algorithms for parameter estimation in photovoltaic modules," *Heliyon*, vol. 7, no. 4, article e06673, 2021.

[11] W. Long, S. Cai, J. Jiao, M. Xu, and T. Wu, "A new hybrid algorithm based on grey wolf optimizer and cuckoo search for parameter extraction of solar photovoltaic models," *Energy Conversion and Management*, vol. 203, article 112243, 2020.

[12] K. Balasubramanian, B. Jacob, K. Priya, K. Sangeetha, N. Rajasekar, and T. S. Babu, "Critical evaluation of genetic algorithm based fuel cell parameter extraction," *Energy Procedia*, vol. 75, pp. 1975–1982, 2015.

[13] M. S. Ismail, M. Moghavvemi, and T. M. I. Mahlia, "Characterization of PV panel and global optimization of its model parameters using genetic algorithm," *Energy Conversion and Management*, vol. 73, pp. 10–25, 2013.

[14] W. Long, W. Zhang, Y. Huang, and Y. Chen, "A hybrid cuckoo search algorithm with feasibility-based rule for constrained structural optimization," *Journal of Central South University*, vol. 21, no. 8, pp. 3197–3204, 2014.

[15] A. Rezaee Jordehi, "Enhanced leader particle swarm optimisation (ELPSO): an efficient algorithm for parameter estimation of photovoltaic (PV) cells and modules," *Solar Energy*, vol. 159, pp. 78–87, 2018.

[16] D. Yousri, D. Allam, M. B. Eteiba, and P. N. Suganthan, "Static and dynamic photovoltaic models' parameters identification using chaotic heterogeneous comprehensive learning particle swarm optimizer variants," *Energy Conversion and Management*, vol. 182, pp. 546–563, 2019.

[17] R. Wang, "Parameter identification of photovoltaic cell model based on enhanced particle swarm optimization," *Sustainability*, vol. 13, no. 2, p. 840, 2021.

[18] S. Li, W. Gong, X. Yan, C. Hu, D. Bai, and L. WangParameter estimation of photovoltaic models with memetic adaptive differential evolution," *Solar Energy*, vol. 190, pp. 465–474, 2019.

[19] D. C. Huynh, L. D. Ho, and M. W. Dunnigan, "Parameter estimation of solar photovoltaic cells using an improved artificial bee colony algorithm," in *Computational Intelligence Methods for Green Technology and Sustainable Development*, Y.-P. Huang, W.-J. Wang, H. A. Quoc, L. H. Giang, and N.-L. Hung, Eds., vol. 1284, pp. 281–292, Springer International Publishing, Cham, 2021.

[20] X. Chen, B. Xu, C. Mei, Y. Ding, and K. Li, "Teaching–learning–based artificial bee colony for solar photovoltaic parameter estimation," *Applied Energy*, vol. 212, pp. 1578–1588, 2018.

[21] L. Xu, L. Bai, H. Bao, and J. Jiang, "Parameter identification of solar cell model based on improved artificial bee colony algorithm," in *2021 13th International Conference on Advanced Computational Intelligence (ICACI)*, pp. 239–244, Wanzhou, China, 2021.

[22] A. Askarzadeh and A. Rezazadeh, "Artificial bee swarm optimization algorithm for parameters identification of solar cell models," *Applied Energy*, vol. 102, pp. 943–949, 2013.

[23] M. A. Awadallah, "Variations of the bacterial foraging algorithm for the extraction of PV module parameters from nameplate data," *Energy Conversion and Management*, vol. 113, pp. 312–320, 2016.

[24] B. Subudhi and R. Pradhan, "Bacterial foraging optimization approach to parameter extraction of a photovoltaic module," *IEEE Transactions on Sustainable Energy*, vol. 9, no. 1, pp. 381–389, 2018.

[25] X. Chen and K. Yu, "Hybridizing cuckoo search algorithm with biogeography-based optimization for estimating photovoltaic model parameters," *Solar Energy*, vol. 180, pp. 192–206, 2019.

[26] J. P. Ram, T. S. Babu, T. Dragicevic, and N. Rajasekar, "A new hybrid bee pollinator flower pollination algorithm for solar PV parameter estimation," *Energy Conversion and Management*, vol. 135, pp. 463–476, 2017.

[27] S. Xu and Y. Wang, "Parameter estimation of photovoltaic modules using a hybrid flower pollination algorithm," *Energy Conversion and Management*, vol. 144, pp. 53–68, 2017.

[28] X. Luo, L. Cao, L. Wang, Z. Zhao, and C. Huang, "Parameter identification of the photovoltaic cell model with a hybrid Jaya-NM algorithm," *Optik*, vol. 171, pp. 200–203, 2018.

[29] K. Yu, B. Qu, C. Yue, S. Ge, X. Chen, and J. Liang, "A performance-guided JAYA algorithm for parameters identification of photovoltaic cell and module," *Applied Energy*, vol. 237, pp. 241–257, 2019.

[30] R. Abbassi, A. Abbassi, A. A. Heidari, and S. Mirjalili, "An efficient salp swarm-inspired algorithm for parameters identification of photovoltaic cell models," *Energy Conversion and Management*, vol. 179, pp. 362–372, 2019.

[31] A. Askarzadeh and L. dos Santos Coelho, "Determination of photovoltaic modules parameters at different operating conditions using a novel bird mating optimizer approach," *Energy Conversion and Management*, vol. 89, pp. 608–614, 2015.

[32] S. J. Patel, A. K. Panchal, and V. Kheraj, "Extraction of solar cell parameters from a single current–voltage characteristic using teaching learning based optimization algorithm," *Applied Energy*, vol. 119, pp. 384–393, 2014.

[33] A. Ramadan, S. Kamel, A. Korashy, and J. Yu, "Photovoltaic cells parameter estimation using an enhanced teaching–learning-based optimization algorithm," *Iranian Journal of Science and Technology, Transactions of Electrical Engineering*, vol. 44, no. 2, pp. 767–779, 2020.

[34] Q. Fan, Y. Zhang, and Z. Wang, "Improved teaching learning based optimization and its application in parameter estimation of solar cell models," *Intelligent Automation and Soft Computing*, pp. 1–12, 2018.

[35] M. Abd Elaziz and D. Oliva, "Parameter estimation of solar cells diode models by an improved opposition- based whale optimization algorithm," *Energy Conversion and Management*, vol. 171, pp. 1843–1859, 2018.

[36] D. Oliva, M. Abd El Aziz, and A. Ella Hassanien, "Parameter estimation of photovoltaic cells using an improved chaotic whale optimization algorithm," *Applied Energy*, vol. 200, pp. 141–154, 2017.

[37] X. Ye, W. Liu, H. Li et al., "Modified whale optimization algorithm for solar cell and PV module parameter identification," *Complexity*, vol. 2021, 23 pages, 2021.

[38] K. Yu, J. J. Liang, B. Y. Qu, Z. Cheng, and H. Wang, "Multiple learning backtracking search algorithm for estimating parameters of photovoltaic models," *Applied Energy*, vol. 226, pp. 408–422, 2018.

[39] H. Chen, S. Jiao, A. A. Heidari, M. Wang, X. Chen, and X. Zhao, "An opposition-based sine cosine approach with local search for parameter estimation of photovoltaic models," *Energy Conversion and Management*, vol. 195, pp. 927–942, 2019.

[40] A. Fathy and H. Rezk, "Parameter estimation of photovoltaic system using imperialist competitive algorithm," *Renewable Energy*, vol. 111, pp. 307–320, 2017.

[41] F. Jabari, M. Mohammadpourfard, and B. Mohammadi-ivatloo, "Energy efficient hourly scheduling of multi-chiller systems using imperialistic competitive algorithm," *Computers and Electrical Engineering*, vol. 82, article 106550, 2020.

[42] E. E. Ali, M. A. El-Hameed, A. A. El-Fergany, and M. M. El-Arini, "Parameter extraction of photovoltaic generating units using multi-verse optimizer," *Sustainable Energy Technologies and Assessments*, vol. 17, pp. 68–76, 2016.

[43] D. Nasri and D. Mokeddem, "Ant lion optimizer for the estimation of photovoltaic (PV) cells parameters," in *Advances in Computing Systems and Applications*, M. R. Senouci, M. E. Y. Boudaren, F. Sebbak, and M. Mataoui, Eds., vol. 199, pp. 85–95, Springer International Publishing, Cham, 2021.

[44] Z. Wu, D. Yu, and X. Kang, "Parameter identification of photovoltaic cell model based on improved ant lion optimizer," *Energy Conversion and Management*, vol. 151, pp. 107–115, 2017.

[45] Z. Chen, L. Wu, P. Lin, Y. Wu, and S. Cheng, "Parameters identification of photovoltaic models using hybrid adaptive

Nelder-Mead simplex algorithm based on eagle strategy," *Applied Energy*, vol. 182, pp. 47–57, 2016.

[46] L. Guo, Z. Meng, Y. Sun, and L. Wang, "Parameter identification and sensitivity analysis of solar cell models with cat swarm optimization algorithm," *Energy Conversion and Management*, vol. 108, pp. 520–528, 2016.

[47] A. Askarzadeh and A. Rezazadeh, "Parameter identification for solar cell models using harmony search-based algorithms," *Solar Energy*, vol. 86, no. 11, pp. 3241–3249, 2012.

[48] A. M. Beigi and A. Maroosi, "Parameter identification for solar cells and module using a hybrid firefly and pattern search algorithms," *Solar Energy*, vol. 171, pp. 435–446, 2018.

[49] P. Lin, S. Cheng, W. Yeh, Z. Chen, and L. Wu, "Parameters extraction of solar cell models using a modified simplified swarm optimization algorithm," *Solar Energy*, vol. 144, pp. 594–603, 2017.

[50] Y. Wu, R. Chen, C. Li, L. Zhang, and Z. Cui, "Hybrid symbiotic differential evolution moth-flame optimization algorithm for estimating parameters of photovoltaic models," *IEEE Access*, vol. 8, pp. 156328–156346, 2020.

[51] D. Kler, P. Sharma, A. Banerjee, K. P. S. Rana, and V. Kumar, "PV cell and module efficient parameters estimation using evaporation rate based water cycle algorithm," *Swarm and Evolutionary Computation*, vol. 35, pp. 93–110, 2017.

[52] P. J. Gnetchejo, S. N. Essiane, P. Ele, R. Wamkeue, D. M. Wapet, and S. P. Ngoffe, "Enhanced vibrating particles system algorithm for parameters estimation of photovoltaic system," *Journal of Power and Energy Engineering*, vol. 7, no. 8, pp. 1–26, 2019.

[53] H. Chen, S. Jiao, M. Wang, A. A. Heidari, and X. Zhao, "Parameters identification of photovoltaic cells and modules using diversification-enriched Harris hawks optimization with chaotic drifts," *Journal of Cleaner Production*, vol. 244, article 118778, 2020.

[54] H. M. Hasanien, "Shuffled frog leaping algorithm for photovoltaic model identification," *IEEE Transactions on Sustainable Energy*, vol. 6, no. 2, pp. 509–515, 2015.

[55] W. Zhou, P. Wang, A. A. Heidari et al., "Metaphor-free dynamic spherical evolution for parameter estimation of photovoltaic modules," *Energy Reports*, vol. 7, pp. 5175–5202, 2021.

[56] I. Ahmadianfar, W. Gong, A. A. Heidari, N. A. Golilarz, A. Samadi-Koucheksaraee, and H. Chen, "Gradient-based optimization with ranking mechanisms for parameter identification of photovoltaic systems," *Energy Reports*, vol. 7, pp. 3979–3997, 2021.

[57] Y. Fan, P. Wang, A. A. Heidari, X. Zhao, H. Turabieh, and H. Chen, "Delayed dynamic step shuffling frog-leaping algorithm for optimal design of photovoltaic models," *Energy Reports*, vol. 7, pp. 228–246, 2021.

[58] Y. Liu, A. A. Heidari, X. Ye et al., "Evolutionary shuffled frog leaping with memory pool for parameter optimization," *Energy Reports*, vol. 7, pp. 584–606, 2021.

[59] X. Weng, A. A. Heidari, G. Liang et al., "Laplacian Nelder-Mead spherical evolution for parameter estimation of photovoltaic models," *Energy Conversion and Management*, vol. 243, article 114223, 2021.

[60] Y. Fan, P. Wang, A. A. Heidari, H. Chen, HamzaTurabieh, and M. Mafarja, "Random reselection particle swarm optimization for optimal design of solar photovoltaic modules," *Energy*, vol. 239, article 121865, 2022.

[61] Y. Liu, A. A. Heidari, X. Ye, G. Liang, H. Chen, and C. He, "Boosting slime mould algorithm for parameter identification of photovoltaic models," *Energy*, vol. 234, article 121164, 2021.

[62] H. A. Alsattar, A. A. Zaidan, and B. B. Zaidan, "Novel meta-heuristic bald eagle search optimisation algorithm," *Artificial Intelligence Review*, vol. 53, no. 3, pp. 2237–2264, 2020.

[63] K. Yu, J. J. Liang, B. Y. Qu, X. Chen, and H. Wang, "Parameters identification of photovoltaic models using an improved JAYA optimization algorithm," *Energy Conversion and Management*, vol. 150, pp. 742–753, 2017.

[64] X. Chen, K. Yu, W. Du, W. Zhao, and G. Liu, "Parameters identification of solar cell models using generalized oppositional teaching learning based optimization," *Energy*, vol. 99, pp. 170–180, 2016.

[65] R. Chenouard and R. A. El-Sehiemy, "An interval branch and bound global optimization algorithm for parameter estimation of three photovoltaic models," *Energy Conversion and Management*, vol. 205, article 112400, 2020.

[66] V. J. Chin and Z. Salam, "A new three-point-based approach for the parameter extraction of photovoltaic cells," *Applied Energy*, vol. 237, pp. 519–533, 2019.

[67] H. Sheng, C. Li, H. Wang et al., "Parameters extraction of photovoltaic models using an improved moth-flame optimization," *Energies*, vol. 12, no. 18, p. 3527, 2019.

[68] T. Huang, C. Zhang, H. Ouyang, G. Luo, S. Li, and D. Zou, "Parameter identification for photovoltaic models using an improved learning search algorithm," *IEEE Access*, vol. 8, article 116292, 116309 pages, 2020.

[69] S. Li, W. Gong, X. Yan et al., "Parameter extraction of photovoltaic models using an improved teaching- learning-based optimization," *Energy Conversion and Management*, vol. 186, pp. 293–305, 2019.

[70] J. J. Liang, S. Zhigang, and L. Zhihui, "Coevolutionary comprehensive learning particle swarm optimizer," in *IEEE Congress on Evolutionary Computation*, pp. 1–8, Barcelona, Spain, July 2010.

[71] R. V. Rao, V. J. Savsani, and D. P. Vakharia, "Teaching–learning-based optimization: an optimization method for continuous non-linear large scale problems," *Information Sciences*, vol. 183, no. 1, pp. 1–15, 2012.

[72] Z. Liao, Z. Chen, and S. Li, "Parameters extraction of photovoltaic models using triple-phase teaching-learning-based optimization," *IEEE Access*, vol. 8, pp. 69937–69952, 2020.